Journal of Molecular Liquids 416 (2024) 126503

Contents lists available at ScienceDirect

Journal of Molecular Liquids

journal homepage: www.elsevier.com/locate/molliq

Tunable optical limiting in silver nanoparticle-naphthophenanthridine hybrids

Mary Joseph [a], Sharon Tomson [b], Marichandran Vadivel [c], K. Swamynathan [c,d], Sandeep Kumar [c,d], Reji Philip [b], Benoy Anand [e,*]

[a] Department of Physics, Christ College (University of Calicut), Irinjalakuda, Kerala 680121, India
[b] Light and Matter Physics Group, Raman Research Institute, Bengaluru 560080, India
[c] Soft Condensed Matter Group, Raman Research Institute, Bengaluru 560080, India
[d] Department of Chemistry, NITTE Meenakshi Instittue of Technology, Gollahalli, Bengaluru 560064, India
[e] Department of Physics, St. Joseph's College (University of Calicut), Irinjalakuda, Kerala 680121, India

ARTICLE INFO

Keywords:
Optical limiting
Naphthophenanthridine
Discotic liquid crystals
Nonlinear optics
Nanosecond laser

ABSTRACT

Incorporation of functional nanoparticles into liquid crystals has emerged as a promising approach to create liquid crystal nanocomposites with superior opto-electronic properties. The properties of self-assembled supramolecular structures change remarkably upon the dispersion of a minute amount of metal nanoparticles in them. The effect of dispersing alkyl thiol-functionalized silver nanoparticles (Ag NP) in Naphthophenanthridine discotic liquid crystals on the nonlinear optical (NLO) properties is discussed in this work. Discotic liquid crystals (DLC) are synthesized via N-annulation of hexabutoxytriphenylene-1-amine with heptanaldehyde through the Pictet–Spengler reaction. A uniform dispersion of about 1–3 wt% Ag NPs in the columnar matrix enhances the nonlinear optical absorption, when measured under excitation by nanosecond laser pulses at 532 nm. By changing the amount of Ag NP loading, the nonlinear response of the hybrid can be tuned. These results indicate that the Ag-DLC hybrids are potential candidates for applications in NLO devices such as tunable optical limiters.

1. Introduction

Optical limiting (OL) is a nonlinear phenomenon in which an optical system having high transmission attenuates light considerably when the input intensity exceeds a certain threshold [1]. Thus, an optical limiter can protect eyes and sensors from the damage caused by intense laser radiation or other bright light sources. Numerous studies done on optical limiting materials have posited that no single material or mechanism can fully meet the stringent requirements for practical applications [1]. Hence there is a need for hybrid structures which can go beyond the capabilities of conventional materials. In this regard nanoparticle-liquid crystal hybrids are emerging to be a promising candidate as they possess excellent nonlinear optical (NLO) properties [2]. Integration of nanoparticles (NP) into liquid crystal matrices gives rise to enhanced optical, electrical, and mechanical characteristics [3–8]. The interplay between nanoparticles and liquid crystals induces synergistic effects, offering avenues for exploitation in diverse technological applications [2,9]. Among nanoparticles, metal nanoparticles such as silver (Ag) and gold, are particularly interesting for NLO applications because of their plasmonic effects, which enhance the local electric field and thereby the nonlinear response [10]. Previously NLO studies done on Ag nanoclusters and oxide-protected Ag NPs showed strong third order nonlinear absorption in the femtosecond and nanosecond (ns) excitation regimes, which is ideal for OL applications [11,12]. Depending on the excitation conditions, the mechanism of NLO behaviour is attributed to nonlinear processes such as two-photon absorption, free carrier absorption, induced thermal scattering etc. Since the optical nonlinearity in Ag NPs depends on various factors such as the size, shape, composition, and local environment of the nanoparticles, controlling these parameters can lead to tunable optical limiting performance [13].

Liquid crystals exhibit versatile optical nonlinearities that render them suitable for photonic applications across a broad temporal and spectral range [14]. These nonlinearities stem from the pronounced anisotropy and highly correlated molecular reorientation of liquid crystals when subjected to external fields [15]. Among various classes of liquid crystals, discotic liquid crystals (DLC) stand out due to their distinctive molecular structure and remarkable properties. Here, disk-shaped molecules stack on top of each other in columns. The extended

* Corresponding author.
E-mail address: anandbenoy@gmail.com (B. Anand).

https://doi.org/10.1016/j.molliq.2024.126503
Received 26 July 2024; Received in revised form 25 October 2024; Accepted 12 November 2024
Available online 14 November 2024

π-electron conjugation along the column axis leads to high polarizability, which is ideal for NLO applications [16]. The electronic structure of DLCs supports robust nonlinear absorption in both the visible and infrared regions [17,18].

Naphthophenanthridine (Nph) is triphenylene-based discotic liquid crystal which forms stable columnar structures *via* intense π–π interactions between the polyaromatic cores. They possess superior charge mobility and optical properties which make them attractive for opto-electronic applications such as organic solar cells, light-emitting diodes, and field-effect transistors [19,20]. The physical properties of discotic triphenylene are highly tunable, as it has been shown that, modifying even one of the peripheral chains on the aromatic core results in drastic changes in the phase behaviour [21,22]. Triphenylene based DLCs have also been widely explored for NLO applications. Gowda *et al.* synthesized symmetrical phenazine-fused-triphenylene derivatives of DLC. The extensive delocalization of π–electrons within discotic mesogens resulted in strong NLO response due to excited state absorption when assessed with nanosecond laser pulses [22]. The present study explores the NLO properties of Naphthophenanthridine discotic liquid crystals (Nph DLC) using open aperture Z-scan technique. Nph DLC shows strong nonlinear absorption in the nanosecond excitation regime due to the extended π-electron conjugation, which results in OL. In an attempt to improve the nonlinear response, hybrid liquid crystal structures are developed by incorporating Ag NPs into the DLC matrix. Strength of nonlinear absorption is found to increase systematically with Ag loading, rendering tunable OL performance.

2. Experimental procedure

2.1. Synthesis

2.1.1. Synthesis of hexanethiol-capped silver nanoparticles

Hexanethiol-capped Ag NPs are synthesized following the literature procedure [23,24]. About 0.2 g of $AgNO_3$ is dissolved in 20 ml of ethanol using a magnetic stirrer. When 0.138 g of 1-hexanethiol is added to the stirring solution at room temperature, a light-yellow cloudy solution appeared, which indicates the formation of silver thiolates. The stirring is continued for one hour at room temperature. A freshly prepared solution of sodium borohydride (0.312 g) in 5 mL of absolute ethanol is added dropwise using a micropipette to the reaction mixture under vigorous stirring. The colour of the solution changes to reddish-brown, indicating the reduction of Ag^+ to metallic silver (Ag (0)). The reaction mixture is stirred for 3 h at room temperature. The mixture is refrigerated overnight and then washed with acetone and water to remove impurities. The NPs are finally filtered, and dried for two days.

2.1.2. Synthesis of Naphthophenanthridine discotic liquid crystals

Hexabutoxytriphenylene (HAT4) is prepared using Scholl reaction following the literature procedure [25,26]. The purified HAT4 is mononitrated by using HNO_3. Then the nitro group is reduced to amine using H_2 in the presence of Raney Nickel. The isolated amine as such is used for the next step. The Pictet-Spengler reaction is carried out with appropriate aldehyde and amine with triflic acid as catalyst in dimethylformamide [27–29]. The final product (Nph DLC) is purified using column chromatography and analysed for its chemical purity before further characterization. The purity and structure of the isolated products are confirmed by ^{1}H NMR,^{13}C NMR, HRMS, and elemental analysis [19,28,29]. The chemical structure of Naphthophenanthridine [29] is given in Fig. 1. The details of synthesis and mesomorphic characterizations are given in the Supplementary information.

2.1.3. Preparation of Ag NP-DLC hybrids

Nanocomposites having weight percentage 1 %, 2 % and 3 % of Ag NPs in Nph DLC are prepared by mixing them in chloroform. Ag NPs are first dissolved in chloroform and the solution is sonicated for 30 min at room temperature. Nph DLC is added to this solution and the sonication continued for another 30 min to achieve homogenous dispersion.

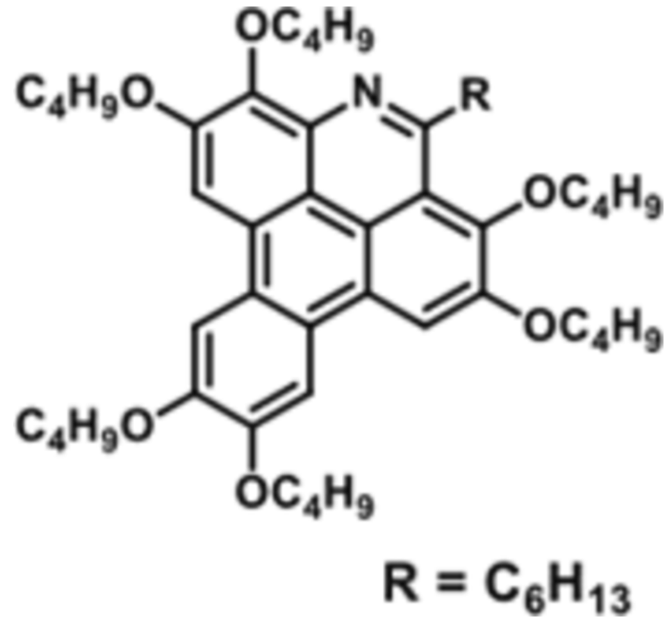

Fig. 1. Chemical structure of Naphthophenanthridine.

2.2. Characterization

Optical absorption studies are carried out by PerkinElmer Lambda 35 double-beam spectrophotometer. HRTEM imaging of Ag NPS is done using JEOL JEM-2100 transmission electron microscope. The presence of nanoparticles on the DLC is characterized by FE-SEM (Ultra Plus, Carl Zeiss).

2.3. Open aperture Z-scan

In order to measure nonlinear absorption in the samples, open aperture Z-scan measurements are carried out using 5 nanosecond (ns) Gaussian pulses of 532 nm from a frequency-doubled Nd:YAG laser. Samples dispersed in chloroform are transferred to a 1 mm thick quartz cuvette. Their concentrations are adjusted such that the linear transmittance at the excitation wavelength is 84 % for the Nph DLC, 80 % for Ag NPs and 75 % for the Ag-DLC hybrids. The cuvette is mounted on a translation stage and the laser pulses are focused on to it using a converging lens, as shown in Fig. 2 (In closed-aperture Z-scan, an additional aperture is positioned in front of the detector D1, which makes it sensitive to changes in beam divergence due to nonlinear refraction). By moving the translation stage along the propagation direction (taken as z-axis), the sample is subjected to an intensity gradient. The intensity dependent transmittance of the sample, recorded using a photodiode, is plotted as a function of the sample position (z). By fitting this Z-scan curve using various pulse propagation equations, relevant NLO parameters are extracted and the underlying mechanism is delineated. Open-aperture Z-scan technique is typically used to study nonlinear absorption, providing information about the imaginary part of susceptibility. On the other hand, closed-aperture Z-scan technique enables the measurement of nonlinear refractive index corresponding to the real part of susceptibility.

3. Results and discussion

3.1. Electron microscopy

Fig. 3a shows the TEM image of hexanethiol-capped Ag NPs. The size distribution of the nanoparticles is shown in the inset. From the Gaussian

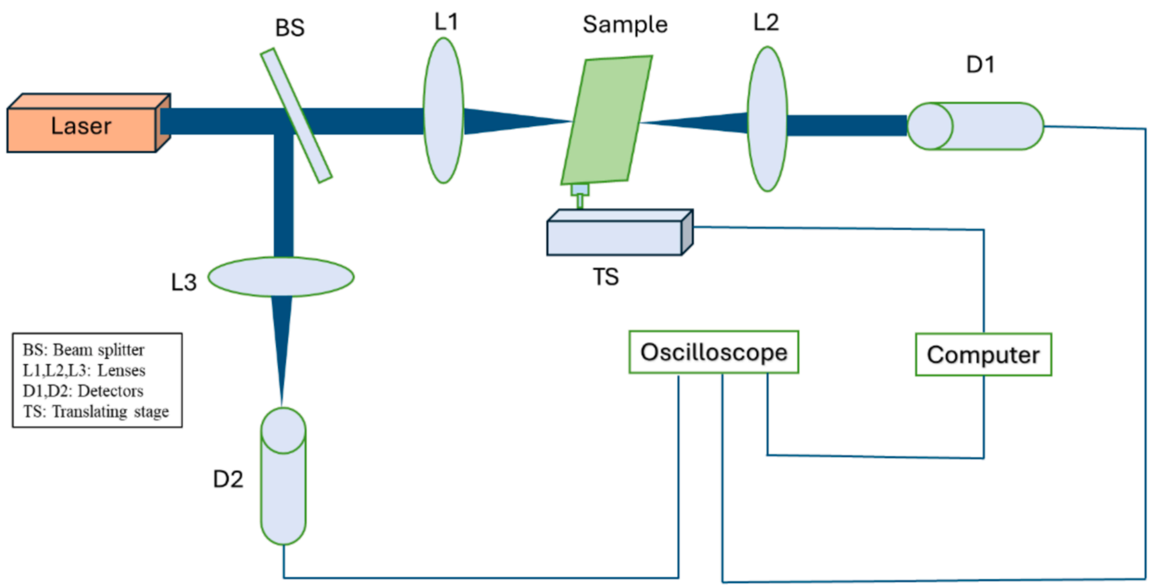

Fig. 2. Schematic of the open-aperture Z-scan setup used for nonlinear absorption measurements.

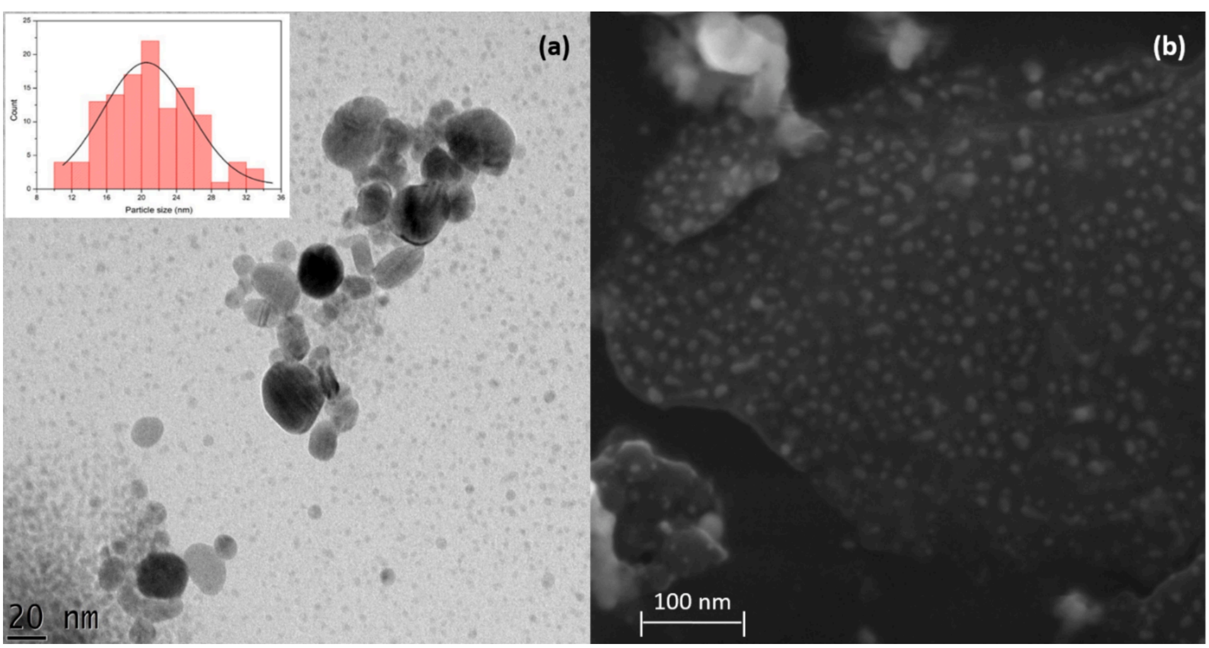

Fig. 3. (a) TEM image of Ag nanoparticles. Inset shows the size distribution with a Gaussian fit. (b) FE-SEM image of Ag-DLC hybrids.

fit, the average diameter of the distribution is found to be 20.5 nm with a standard deviation of ±5 nm. The FE-SEM image of the Ag-DLC hybrids shown in Fig. 3b confirms a uniform distribution of the nanoparticles on the surface of the DLC.

3.2. Linear absorption studies

The UV–Visible absorption spectrum of the Ag NPs suspended in chloroform given in Fig. 4a shows characteristic surface plasmon peak at 419 nm. Plasmon peak of nanoparticles is sensitive to the surface properties, size of the particle and nature of the capping layer. The absorption spectra of Nph DLC and Ag-DLC hybrids (Fig. 4b) show peaks ranging from 263 nm to 383 nm, with the strongest peak located at 263 nm. The absorption between 260 nm and 285 nm is assigned to π–π* transition from the π-electrons of central naphthophenanthridine core, and the peak at 383 nm corresponds to n-π* transitions from the lone-pair of electrons of the heteroatom in the system. All the hybrids show the characteristic absorption peaks of DLC. No additional peaks or shift in existing peaks is observed upon the incorporation of Ag nanoparticles into the DLC matrix. This is probably due to the low weight percentage of the nanoparticles [23].

3.3. Nonlinear optical studies

Open aperture Z-scan measurements carried out on Nph DLC and its metal hybrids show strong nonlinear absorption in the ns excitation

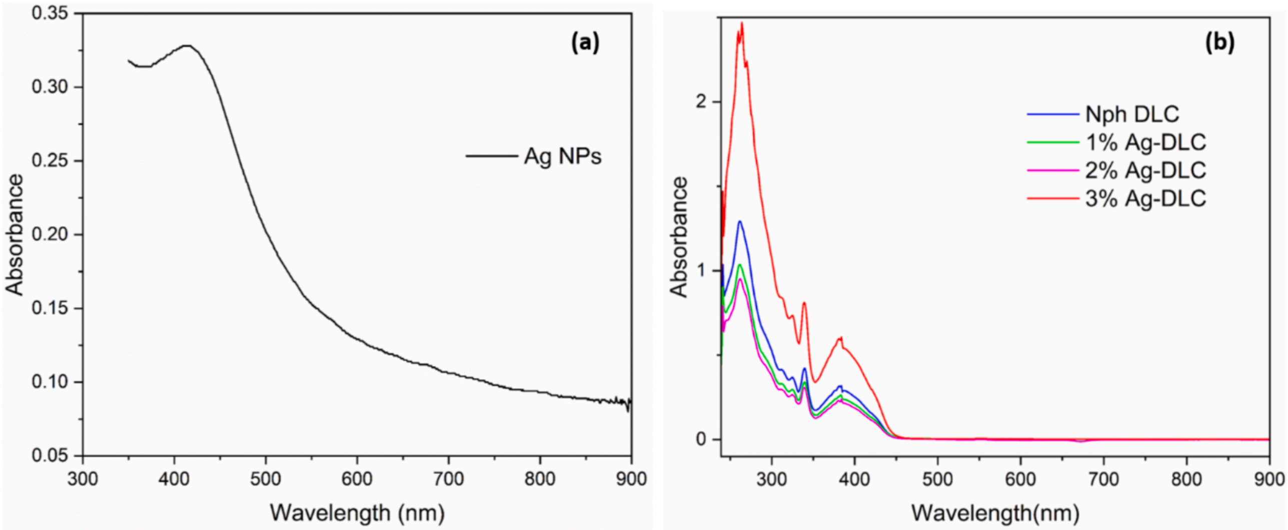

Fig. 4. UV–Vis absorption spectra of (a) Ag nanoparticles and, (b) naphthophenanthridine DLC and Ag-DLC nanocomposites.

regime (Fig. 5b). The intensity gradient generated during the Z-scan experiment peaks near the laser focus (denoted as z = 0) and decreases on either side as z increases. Reduction in sample transmittance near the focus seen in Fig. 5b indicates an increase in light absorption due to increase in intensity. Such a reverse saturable absorption (RSA) behaviour is important for NLO applications such as OL [30]. To understand the mechanism of nonlinear absorption, Z-scan data is numerically fitted with different pulse propagation equations. For theoretically simulating the sample transmission, intensity of the Gaussian beam is calculated using the laser pulse energy, pulse width and irradiation area. The intensity is then integrated over time to calculate the corresponding fluence. Nonlinear transmittance of a given sample is obtained by dividing the output fluence with the input fluence. For comparing the transmission characteristics of different samples, the transmittance is normalized with the linear transmittance, thereby yielding the normalized transmittance.

For Nph DLC, the best fit is obtained with a two-photon absorption (2PA) model, as shown in Fig. 6a, wherein the intensity dependent absorption coefficient α is given as $\alpha(I) = \alpha_o + \beta I$ [31]. Here I is the laser intensity, α_o is the linear absorption coefficient and β is the 2PA coefficient. Transmission characteristics are simulated by numerically solving the 2PA propagation equation $\frac{dI}{dz'} = -\alpha_o I - \beta I^2$, where z' is the propagation distance within the sample. Value of 2PA coefficient β obtained from the best fit is 1×10^{-10} m/W for a pulse energy of 90 μJ. This is comparable to the nonlinear absorption measured under similar ns laser excitation conditions in materials such as Se and Te nanowires, Bi nanorods, PbS microtowers, etc. [32].

Nonlinear absorption measured in Ag NPs arises due to two competing processes: saturable absorption (SA) and reverse saturable absorption. SA occurs when the material's absorption decreases with increasing intensity near the laser focus (z = 0), which appears as a peak (increase in transmittance) in the open-aperture Z-scan graph. Whereas, RSA appears as a valley (decrease in transmittance), as mentioned before. At high pulse energies (>60 μJ), transmission behaviour of Ag NPs is dictated by reverse saturable absorption, as shown in Fig. 5a (small humps on either side of the focus indicate a weak saturation behaviour). Since there is an interplay between two different nonlinear processes, the best fit is obtained with a 2PA + SA model (Fig. 6b) described by the propagation equation $\frac{dI}{dz'} = -\frac{\alpha_o I}{1+I/I_s} - \beta I^2$ where I_s is the saturation intensity (at which the linear absorption coefficient drops to half its original value). Correspondingly, the absorption coefficient gets modified as $\alpha(I) = \frac{\alpha_o}{1+I/I_s} + \beta I$ [31]. It is well known that the plasmon band of metal nanoparticles arises from the collective oscillations of the free electrons near the Fermi level. SA observed at lower pulse energies in Ag nanoparticles arises due to the bleaching of this ground-state plasmon

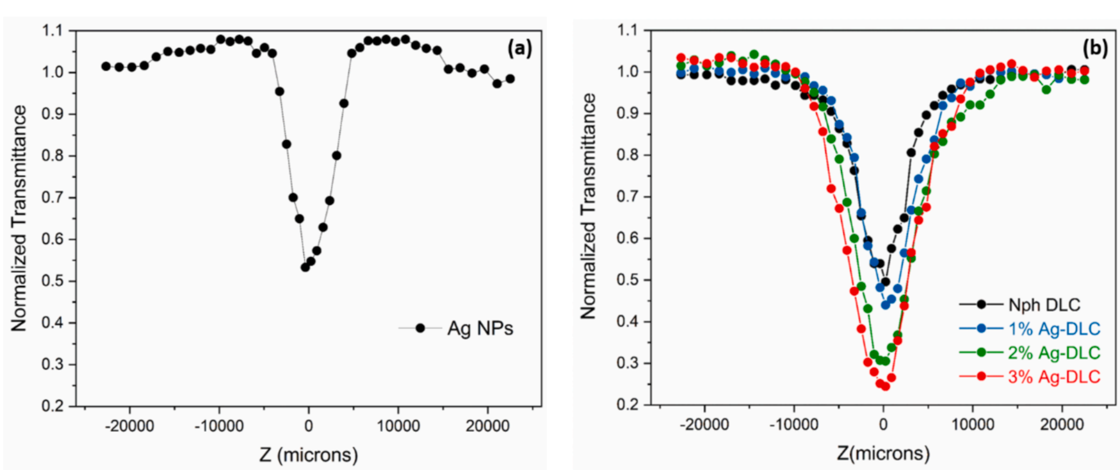

Fig. 5. Open aperture Z-scan curves of (a) Ag nanoparticles, and (b) naphthophenanthridine DLC and Ag-DLC hybrids measured with 5 ns laser pulses of 90 μJ pulse energy at the excitation wavelength of 532 nm.

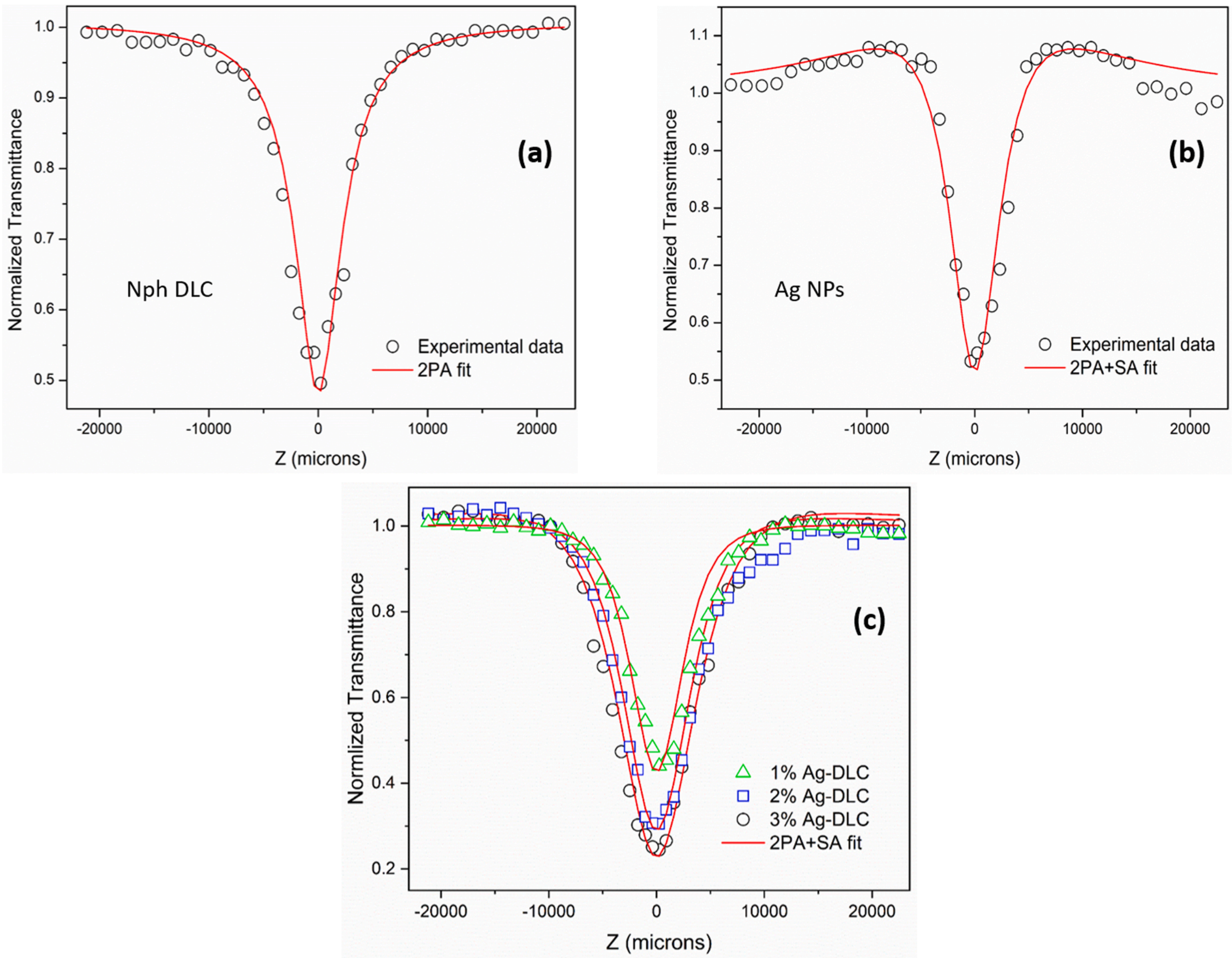

Fig. 6. Open aperture Z-scan curves of (a) Nph DLC fitted with 2PA model, (b) Ag NPs fitted with 2PA + SA model, and (c) Ag-DLC hybrids fitted with 2PA + SA model. The symbols represent experimental data measured with 5 ns laser pulses of 90 µJ pulse energy at the excitation wavelength of 532 nm and the red solid line represents the theoretical fit.

band [33]. In brief, when subjected to a laser pulse, metal nanoparticles can undergo interband or intraband electron transitions depending on the excitation wavelength and intensity. This process results in the diminishment of the ground-state plasmon band, referred to as 'bleach'. The electrons excited in this manner are called free carriers as they possess a wide spectrum of energies immediately after the absorption. At high pulse energies or intensities, these free carriers absorb additional photons and make transitions to even higher energy states. Absorption of multiple photons through free carrier absorption results in RSA.

Depth of the open-aperture Z-scan curve is a measure of the strength of nonlinear absorption. Therefore, it is clear from Fig. 5b that nonlinear absorption of Nph DLC enhances upon Ag loading. This is primarily due to the strong nonlinear absorption in Ag nanoparticles. Consequently, the Z-scan data of Ag-DLC hybrids are best fitted to a 2PA + SA model (Fig. 6c), rather than a 2PA model. Absorption spectrum of Ag NPs given in Fig. 4a show sufficient absorption at the excitation wavelength of 532 nm. At low pulse energies (<30 µJ), the energy levels corresponding to 532 nm (2.33 eV) gets filled easily. The SA component of nonlinear absorption in the hybrids arises due to the saturation of absorption transition at 532 nm. When pulse energy or intensity increases (>60 µJ), higher order processes like excited state absorption and free carrier absorption become more and more likely. Here, an electron which is already in the first excited state (2.33 eV) absorbs another photon of wavelength 532 nm and gets excited to the second excited state (4.66 eV). This results in an 'effective' 2PA behaviour [34]. In pure 2PA, two photons are absorbed simultaneously; whereas in the case of 'effective' 2PA, both the photons are absorbed sequentially. NLO parameter listed in Table 1 reveal that the strength of nonlinear absorption (indicated by the value of β) in the hybrids increases as a function of Ag loading. Due to the broadband nature of free carrier absorption, Ag-DLC hybrids hold great promise for the development of fast, broadband optical limiters. By controlling the amount of Ag loading, the OL performance can be tuned. Additionally, the rapid recovery of the ground-state plasmon band bleach, typically occurring within picoseconds, positions them as promising candidates for optical switching applications [32].

Table 1
NLO parameters extracted from the best fit curves for various samples. Strength of nonlinear absorption increases with Ag loading.

Sample Name	Laser pulse energy	2PA coefficient (β)	Saturation intensity (I_s)
Nph DLC	90 µJ	1×10^{-10} m/W	
Ag NPs	90 µJ	4×10^{-11} m/W	1×10^{12} W/m^2
1 % Ag-DLC	90 µJ	6×10^{-11} m/W	6×10^{12} W/m^2
2 % Ag-DLC	90 µJ	1.1×10^{-10} m/W	1.5×10^{12} W/m^2
3 % Ag-DLC	90 µJ	1.5×10^{-10} m/W	9×10^{11} W/m^2

4. Conclusions

Silver hybrids of naphthophenanthridine discotic liquid crystals have been prepared by incorporating 1–3 wt% of Ag nanoparticles. The presence of NPs on the surface of DLCs is verified using FE-SEM. Upon excitation with 5 ns laser pulses of 532 nm, Nph DLC exhibits robust nonlinear absorption. Through theoretical modelling, the mechanism of nonlinear absorption process is attributed to two-photon absorption. The strength of nonlinear absorption demonstrates a systematic increase with the loading of Ag NPs, owing to the pronounced free carrier absorption within the Ag component. Theoretical analysis reveals that the mechanism involves an interplay between two-photon absorption and saturable absorption, rendering these hybrids as promising candidates for applications like optical limiting and optical switching. Thus, our study demonstrates that tailoring of liquid crystal properties using metal nanoparticles is a successful approach for the development of tunable NLO devices.

CRediT authorship contribution statement

Mary Joseph: Writing – original draft, Investigation, Formal analysis, Data curation. **Sharon Tomson:** Investigation. **Marichandran Vadivel:** Investigation. **K. Swamynathan:** Writing – original draft, Supervision, Funding acquisition, Investigation. **Sandeep Kumar:** Writing – review & editing, Writing – original draft. **Reji Philip:** Writing – review & editing, Writing – original draft. **Benoy Anand:** Writing – review & editing, Writing – original draft, Visualization, Validation, Supervision, Project administration, Conceptualization.

Declaration of competing interest

The authors declare that they have no known competing financial interests or personal relationships that could have appeared to influence the work reported in this paper.

Acknowledgments

Benoy Anand acknowledges DST-FIST (SR/FST/COLLEGE/2023/1354) and DST-CURIE (DST/CURIE-PG/2023/33) support to St Joseph's College, Irinjalakuda. Swamynathan K. thank Nitte Meenakshi Institute of Technology and Raman Research Institute for the seed money and research facilities respectively.

Appendix A. Supplementary material

Supplementary data to this article can be found online at https://doi.org/10.1016/j.molliq.2024.126503.

Data availability

Data will be made available on request.

References

[1] L.W. Tutt, T.F. Boggess, A review of optical limiting mechanisms and devices using organics, fullerenes, semiconductors and other materials, Prog. Quantum Electron. 17 (1993) 299–338, https://doi.org/10.1016/0079-6727(93)90004-S.

[2] H.K. Bisoyi, S. Kumar, Liquid-crystal nanoscience: an emerging avenue of soft self-assembly, Chem. Soc. Rev. 40 (2011) 306–319, https://doi.org/10.1039/B901793N.

[3] Supreet, G. Singh, Recent advances on cadmium free quantum dots-liquid crystal nanocomposites, Appl. Mater. Today 21 (2020) 100840, https://doi.org/10.1016/j.apmt.2020.100840.

[4] A. Kumar, H. Meena, J. Prakash, L. Wang, G. Singh, Recent advances on semiconducting nanomaterials–ferroelectric liquid crystals nanocomposites, J. Phys. Condens. Matter 34 (1) (2021) 013004, https://doi.org/10.1088/1361-648X/ac2ace.

[5] A. Parveen, J. Prakash, G. Singh, Impact of strontium titanate nanoparticles on the dielectric, electro-optical and electrical response of a nematic liquid crystal, J. Mol. Liq. 354 (2022) 118907, https://doi.org/10.1016/j.molliq.2022.118907.

[6] A. Kumar, G. Singh, Recent advances and future perspectives of photoluminescent liquid crystals and their nanocomposites for emissive displays and other tunable photonic devices, J. Mol. Liq. 386 (2023) 122607, https://doi.org/10.1016/j.molliq.2023.122607.

[7] D. Varshney, K. Yadav, J. Prakash, H. Meena, G. Singh, Tunable dielectric and memory features of ferroelectric layered perovskite Bi4Ti3O12 nanoparticles doped nematic liquid crystal composite, J. Mol. Liq. 369 (2023) 120820, https://doi.org/10.1016/j.molliq.2022.120820.

[8] P. Priscilla, S. Kumar, A.K. Gathania, A.K. Singh, J. Prakash, S. Kumar, P. Malik, R. Castagna, G. Singh, Effect of carbon dots on tuning molecular alignment, dielectric and electrical properties of a smectogenic cyanobiphenyl-based liquid crystal material, J. Phys. D: Appl. Phys. 57 (35) (2024) 355302, https://doi.org/10.1088/1361-6463/ad4a84.

[9] A. Roy, B.P. Singh, G. Yadav, H. Khan, S. Kumar, A. Srivastava, R. Manohar, Effect of gold nanoparticles on intrinsic material parameters and luminescent characteristics of nematic liquid crystals, J. Mol. Liq. 295 (2019) 111872, https://doi.org/10.1016/j.molliq.2019.111872.

[10] Y. Zhang, Y. Wang, Nonlinear optical properties of metal nanoparticles: a review, RSC Adv. 7 (2017) 45129–45144, https://doi.org/10.1039/C7RA07551K.

[11] B. Karthikeyan, J. Thomas, R. Philip, Optical nonlinearity in glass-embedded silver nanoclusters under ultrafast laser excitation, Chemi. Phys. Lett. 414 (2005) 346–350, https://doi.org/10.1016/j.cplett.2005.08.112.

[12] M. Anija, J. Thomas, N. Singh, A. Sreekumaran Nair, R.T. Tom, T. Pradeep, R. Philip, Nonlinear light transmission through oxide-protected Au and Ag nanoparticles: an investigation in the nanosecond domain, Chemi. Phys. Lett. 380 (2003) 223–229, https://doi.org/10.1016/j.cplett.2003.09.023.

[13] P.C. Ray, Size and shape dependent second order nonlinear optical properties of nanomaterials and their application in biological and chemical sensing, Chem. Rev. 110 (2010) 5332–5365, https://doi.org/10.1021/cr900335q.

[14] I.C. Khoo, Nonlinear optics of liquid crystalline materials, Phys. Rep. 471 (2009) 221–267, https://doi.org/10.1016/j.physrep.2009.01.001.

[15] B.Y. Zel'dovich, N.V. Tabiryan, Orientational optical nonlinearity of liquid crystals, Sov. Phys. Usp. 28 (1985) 1059–1083, https://doi.org/10.1070/PU1985v028n12ABEH003985.

[16] D.R. Vinayakumara, M. Kumar, P. Sreekanth, R. Philip, S. Kumar, Synthesis, characterization and nonlinear optical studies of novel blue-light emitting room temperature truxene discotic liquid crystals, RSC Adv. 5 (2015) 26596–26603, https://doi.org/10.1039/C5RA00873E.

[17] S. Laschat, A. Baro, N. Steinke, F. Giesselmann, C. Hägele, G. Scalia, R. Judele, E. Kapatsina, S. Sauer, A. Schreivogel, M. Tosoni, Discotic liquid crystals: from tailor-made synthesis to plastic electronics, Angew. Chem. Int. Ed. 46 (2007) 4832–4887, https://doi.org/10.1002/anie.200604203.

[18] T. Wöhrle, I. Wurzbach, J. Kirres, A. Kostidou, N. Kapernaum, J. Litterscheidt, J. C. Haenle, P. Staffeld, A. Baro, F. Giesselmann, S. Laschat, Discotic liquid crystals, Chem. Rev. 116 (2016) 1139–1241, https://doi.org/10.1021/acs.chemrev.5b00190.

[19] M. Vadivel, S. Singh, D.P. Singh, V.A. Raghunathan, S. Kumar, Ambipolar charge transport properties of naphthophenanthridine discotic liquid crystals, J. Phys. Chem. B 125 (2021) 10364–10372, https://doi.org/10.1021/acs.jpcb.1c06009.

[20] A. Shah, D.P. Singh, B. Duponchel, F. Krasisnski, A. Daoudi, S. Kumar, R. Douali, Molecular ordering dependent charge transport in π-stacked triphenylene based discotic liquid crystals and its correlation with dielectric properties, J. Mol. Liq. 342 (2021) 117353, https://doi.org/10.1016/j.molliq.2021.117353.

[21] J.A. Rego, S. Kumar, H. Ringsdorf, Synthesis and characterization of fluorescent, low-symmetry triphenylene discotic liquid crystals: tailoring of mesomorphic and optical properties, Chem. Mater. 8 (1996) 1402–1409, https://doi.org/10.1021/cm950582x.

[22] A. Kettner, J.H. Wendorff, Modifications of the mesophase formation of discotic triphenylene compounds by substituents, Liq. Cryst. 26 (1999) 483–487, https://doi.org/10.1080/026782999204912.

[23] A.N. Gowda, M. Kumar, A.R. Thomas, R. Philip, S. Kumar, Self-assembly of silver and gold nanoparticles in a metal-free phthalocyanine liquid crystalline matrix: structural, thermal, electrical and nonlinear optical characterization, ChemistrySelect 1 (2016) 1361–1370, https://doi.org/10.1002/slct.201600122.

[24] P. Tripathi, M. Mishra, S. Kumar, R. Dabrowski, R. Dhar, Dependence of physical parameters on the size of silver nano particles forming composites with a nematic liquid crystalline material, J. Mol. Liq. 268 (2018) 403–409, https://doi.org/10.1016/j.molliq.2018.07.046.

[25] J. Wei, B. Han, Q. Guo, X. Shi, W. Wang, N. Wei, 1,5,9-Triazacoronenes: a family of polycyclic heteroarenes synthesized by a threefold Pictet–Spengler reaction, Angew. Chem. Int. Ed. 49 (2010) 8209–8213, https://doi.org/10.1002/anie.201002369.

[26] R.J. Bushby, N. Boden, C.A. Kilner, O.R. Lozman, Z. Lu, Q. Liu, M.A. Thornton-Pett, Helical geometry and liquid crystalline properties of 2,3,6,7,10,11-hexaalkoxy-1-nitrotriphenylenes Electronic supplementary information (ESI) available: calculation of dipolar interactions, details of syntheses and analytical data, DSC data, and full details of the single-crystal structure factors plus projections along the crystallographic axes. See http://www.rsc.org/suppdata/jm/b2/b211133k/, J. Mater. Chem. 13 (2003) 470–474, https://doi.org/10.1039/b211133k.

[27] A.R. Yuvaraj, A. Renjith, S. Kumar, Novel electron-deficient phenanthridine based discotic liquid crystals, J. Mol. Liq. 272 (2018) 583–589, https://doi.org/10.1016/j.molliq.2018.09.120.

[28] M. Vadivel, I.S. Kumar, K. Swamynathan, V.A. Raghunathan, S. Kumar, Novel annulated triphenylene discotic liquid crystals generated by Pictet-Spengler cyclization, ChemistrySelect 3 (2018) 8763–8769, https://doi.org/10.1002/slct.201801738.
[29] M. Vadivel, T. Aravinda, K. Swamynathan, B.V. Kumar, S. Kumar, DNA binding activity of novel discotic phenathridine derivative, J. Mol. Liq. 332 (2021) 115798, https://doi.org/10.1016/j.molliq.2021.115798.
[30] B. Anand, S.R. Krishnan, R. Podila, S. Siva Sankara Sai, A.M. Rao, R. Philip, The role of defects in the nonlinear optical absorption behavior of carbon and ZnO nanostructures, Phys. Chem. Chem. Phys. 16 (2014) 8168, https://doi.org/10.1039/c3cp55334e.
[31] R.L. Sutherland, Handbook of Nonlinear Optics, 0 ed., CRC Press, 2003, doi: 10.1201/9780203912539.
[32] K. Sridharan, M.S. Ollakkan, R. Philip, T.J. Park, Non-hydrothermal synthesis and optical limiting properties of one-dimensional Se/C, Te/C and Se–Te/C core–shell nanostructures, Carbon 63 (2013) 263–273, https://doi.org/10.1016/j.carbon.2013.06.079.
[33] R. Philip, G.R. Kumar, N. Sandhyarani, T. Pradeep, Picosecond optical nonlinearity in monolayer-protected gold, silver, and gold-silver alloy nanoclusters, Phys. Rev. B 62 (2000) 13160–13166, https://doi.org/10.1103/PhysRevB.62.13160.
[34] M. Rumi, J.W. Perry, Two-photon absorption: an overview of measurements and principles, Adv. Opt. Photon. 2 (2010) 451, https://doi.org/10.1364/AOP.2.000451.